Proceedings of the Sixth International Conference on
Railway Technology: Research, Development and Maintenance
Edited by: J. Pombo
Civil-Comp Conferences, Volume 7, Paper 5.11
Civil-Comp Press, Edinburgh, United Kingdom, 2024
ISSN: 2753-3239, doi: 10.4203/ccc.7.5.11

Experimental Investigation of the Track Dynamic Performance for a Downslope Small-Radius Curve in a Metro

X. Liu, H. Jiang, Y. Chen and M. Gao

China Academy of Railway Sciences (Shenzhen) Research and Design Institute Co. Ltd., China Academy of Railway Sciences Corporation Limited
Beijing, China

Abstract

This paper presents the investigation of the track dynamic performance in a typical downslope small-radius curve of a metro line. The rail corrugation and the dynamic performance of the track are analyzed based on the in-site measurement and compared with the upslope side. It has been found that the rail corrugations are mainly developed on the downslope side, and the inner rail has multiple wavelengths from 26 mm to 50 mm. Such a phenomenon is likely to be caused by the complex wheel-rail interaction in the downslope section, where the speed limit requires intermittent braking of the train. The knock-on effect of rail corrugation is rather serious. It not only increased vibration source intensity (on the tunnel wall) of up to 10 dB but also abrupt failure of clips due to resonance. This study has important guiding significance in the design and operation of the metro. Downslope small-radius curves should be avoided in the phase of design. For the existing lines, the speed control mechanism in downslope curves needs to be further optimized to guarantee the smoothness of trains passing through.

Keywords: rail corrugation, metro line, downslope small-radius curve, clip resonance fracture, vibration propagation, excitation frequency.

1 Introduction

Accompanied by the fast urbanization progress, metro lines are rapidly constructed in large cities in China to alleviate traffic congestion. By the end of 2023, the total length

of metro lines in China has reached 8547.67 km. Due to the space limit in these large cities, metro lines are usually laid by underground tunnels and small-radius (R<1000 m) curves are quite common. In some cases, such curves are superimposed with vertical curves (downslope on one side and upslope on the other side). With the growth of the metro service life, the drawbacks of such small-radius curves are gradually exposed.

According to the review by Y. Sato et al.[1] and X. Jin et al.[2], rail corrugation is a prevalent type of damage in the wheel-rail system. The observation and research on rail corrugation has lasted more than a century since the first discovery of such a problem in 1895. In recent years, the rail corrugation problems in small-radius curves have attracted increasingly more attention from researchers and track managers. A. Saulot et al. investigated the damage mechanism of low rail corrugation on sharply curved tracks[3]. It is pointed out that the existence of a rapid inversion in the lateral displacement of the railhead is the main inducement of low rail corrugation. Based on the full-scale tests, in-site experiments and numerical simulation, A. Matsumoto et al. analysed the growing process of rail corrugation in the curve section[4]. It has been found that the stick–slip vibration between the wheel and rail is caused by the large creepage and vertical force fluctuation on the wheel/rail contact surface. Z. Wang and Z. Lei et al.[5]-[7] investigated the formation mechanism of rail corrugation in small radius curves and pointed out that short wavelength corrugation played a dominant role in such sections.

It has to be noted that in the present studies, the vertical curve is rarely considered. The vertical curves have a dramatic influence on the development of the rail damage. Compared with the upslope side, a lot more track damage, such as rail corrugation, appears on the downslope side. The rail corrugation usually results in a dramatic increase of wheel-rail contact forces and may lead to the fracture of clips in extreme cases. Moreover, the ground-born vibration propagated from the metro may also be increased. To investigate the characteristics of rail corrugation and vibration propagation, two sections of small-radius curves with different track types in a metro line are measured. The track conditions of both the downslope sides and the upslope sides are inspected, and the dynamic responses of the rail, the clip and the tunnel wall are analyzed, as presented in this paper below.

2 Methodology

This study is based on in-site measurement and analysis. The rail corrugations are measured using the Corrugation Analysis Trolley (CAT). The key component of the CAT instrument is the measuring head that runs on the rail crown, and the irregularities of the rail can be recorded in the laptop connected to the CAT instrument. The rail corrugation measurement using CAT is shown in Figure 1.

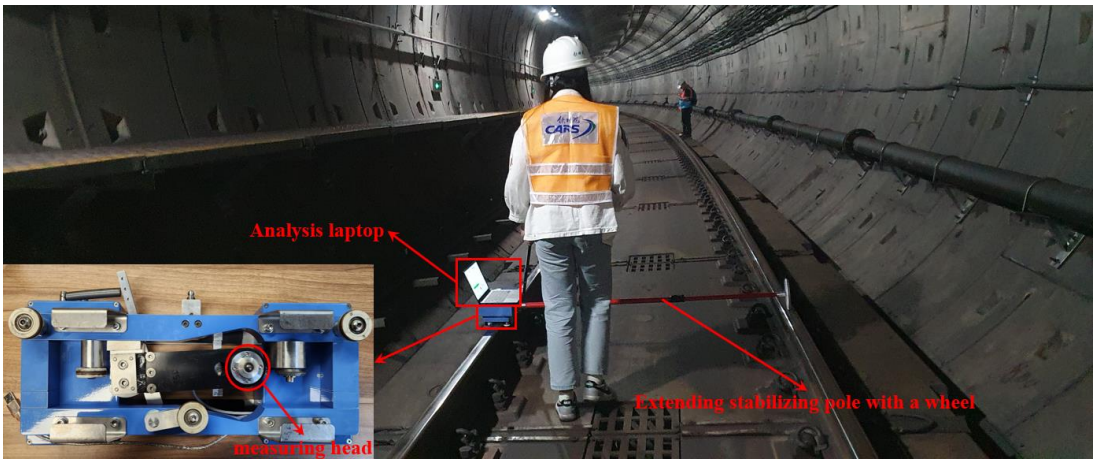

Figure 1: Rail corrugation measurement with CAT.

The dynamic performance of the track is measured using the offline data collection system. When a train passes by, the tunnel wall vertical acceleration (1.25 m above the top of the rail), the rail vertical acceleration (rail bottom between two sleepers) and the clip vertical accelerations (one on the toe-end and another on the small arc) are measured and recorded. The data collection system and the installation of the accelerometers are demonstrated in Figure 2.

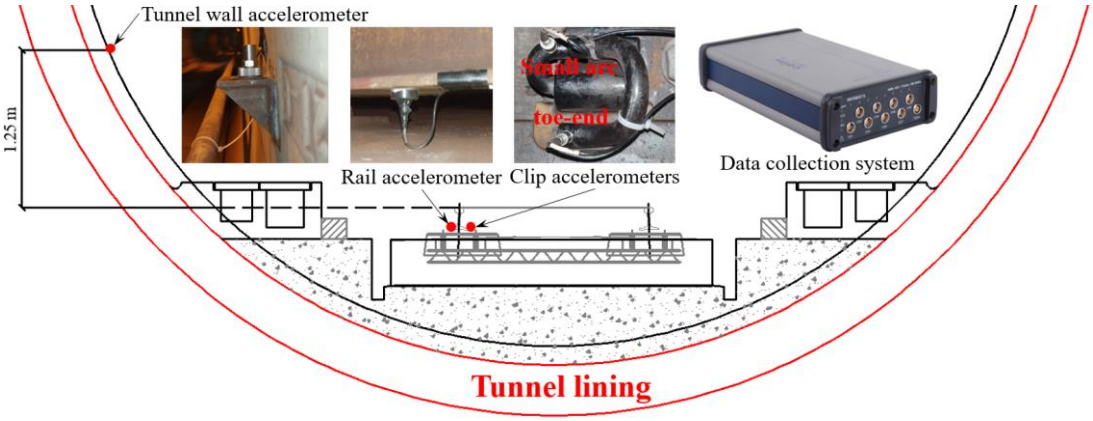

Figure 2: Setup of track vibration test points.

The dynamic performance of the rail and clip is assessed using the measured acceleration responses and analyzed in both the time and frequency domains to investigate the connection with rail corrugation.

For the tunnel wall vibration, the vibration density is assessed using the maximum vibration acceleration level in 1/3 octave spectra ($VL_{\max}$) in the range of 4-200 Hz. The vibration acceleration level can be calculated through formula (1).

$$VL = 20\lg\frac{a}{a_0} \tag{1}$$

Where a is the effective acceleration value, and a_0 is the reference acceleration value.

For train-induced vibration, $a_0=10^{-6}$ m/s^2. For discrete data, the effective acceleration value can be calculated through formula (2):

$$a = \sqrt{\frac{1}{n}(\sum_{j=1}^{n} a_j^2)} \tag{2}$$

Where n is the data length of the measured discrete acceleration signal. The maximum acceleration level in 1/3 octave division ($VL_{\max}$) can be calculated through formula (3):

$$VL_{\max} = \max_{k=1\to n}(VL_k + w_k) \tag{3}$$

Where VL_k is the vibration acceleration level in each 1/3 octave frequency band, and w_k is the corresponding weighting factor. The recommended values of w_k in 4-200 Hz are provided in ISO 2631-1:1997[8] (Table 1). The value of $VL_{\max}$ corrects to an integer by rounding.

1/3 Octave frequency (Hz)	4	5	6.3	8	10	12.5	16	20	25
w_k (dB)	0	0	0	0	0	-1	-2	-4	-6
1/3 Octave frequency (Hz)	31.5	40	50	63	80	100	125	160	200
w_k (dB)	-8	-10	-12	-14	-17	-21	-25	-30	-36

Table 1: Weighting factors in 4-200 Hz are provided in ISO 2631-1:1997.

3 Measurement results and analysis

This study is carried out in a small-radius curve section in a typical metro line in a tunnel. In this section, several track problems are reported, including rail corrugation, broken clips, as well as vibration, propagated to the adjacent vibration-sensitive buildings. Therefore, the objective of this study is to figure out the main causes of these problems and propose reasonable solutions.

The train type operated on this line is the A-type metro train with 8-wagon marshalling. The maximum operation speed is 80 km/h. The information on the instrumented track section is given in the table below.

Direction	Slab type	Curve radius	Slope direction	Slope gradient	Clip type	Corrugation
Left line Right line	Steel-spring floating slab	R=400 m	Downslope Upslope	5 ‰	DT-III	Yes No

Table 2: Information of the instrumented track section.

The track dynamic responses as well as the rail corrugation of the left line are measured both before and after grinding of the rail. The right line has no rail corrugation and the measurement results are to be used as a reference for the assessment of the impact of rail corrugation. The measurement results and analysis are presented in this section below.

3.1 Rail corrugation

Before the measurement of the left line, the rail corrugations are first inspected, as

shown in Figure 3. It can be seen that the corrugation on both the inner rail and the outer rail is visible. The difference is that the outer rail has only one dominant wave with a wavelength of around 50 mm. While on the inner rail, the corrugation is more complicated with several different waves from around 20 mm to 50 mm.

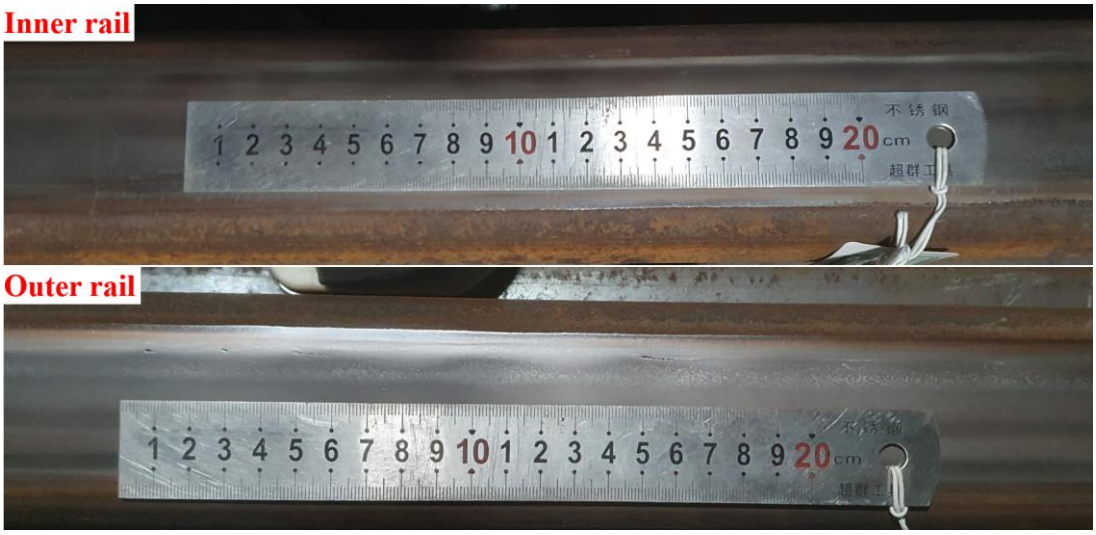

Figure 3: Inspection of rail corrugation in the left line.

Based on the visual inspection, the measuring head of CAT (Figure 1) is adjusted to the middle to measure the major waves of the rail corrugations on both sides. The rail corrugation measurement results are shown in Figure 4.

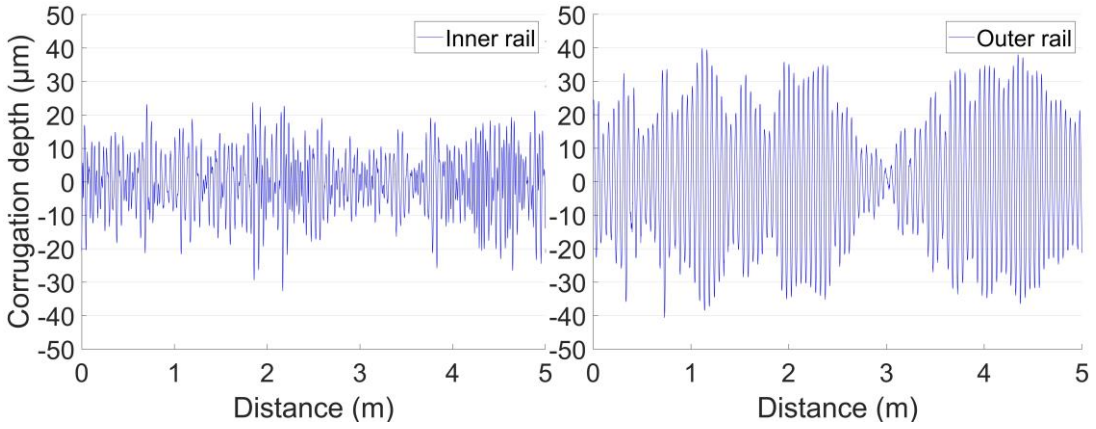

Figure 4: Rail corrugation with the wavelength of 0-100 mm.

It can be seen from Figure 4 that the rail corrugation on the inner rail is shallower and more irregular than that on the outer rail. The maximum depth of the corrugation on the inner rail is around 50 μm, which is around 80 μm on the outer rail.

To precisely assess the wavelength of the corrugation, the measurement data are firstly processed using Fourier transform function, and then take the reciprocal of the independent variables. Finally, the distribution curves of corrugation wavelength are obtained, as presented in Figure 5. It is indicated that the inner rail corrugation has four different wavelengths (λ), which are respectively 26 mm, 33 mm, 4 3mm and 50mm.

$$f_e = v / \lambda \tag{4}$$

The train velocity in this section is v=67 km/h (18.7 m/s). According to formula (4), the excitation frequencies (f_e) of the inner rail corrugation are 719 Hz, 535 Hz, 435 Hz and 374 Hz, respectively. On the outer rail, there is only one main corrugation wavelength of 50 mm (f_e=374 Hz), which is consistent with the longest wave on the inner rail.

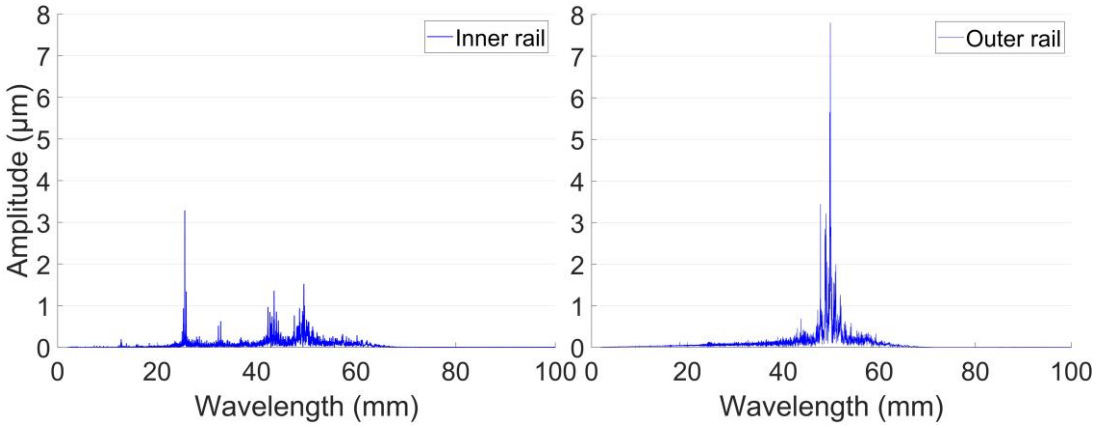

Figure 5: Rail corrugation 0-100 mm wavelength distribution curve.

In this line, the rail is 60 kg/m and the sleeper spacing is 0.6 m, so the corresponding typical pinned-pinned frequency is around 1000 Hz[9]. According to S.L. Grassie[10], the 43 mm and 50 mm corrugations are likely to be caused by the second torsional resonance of driven axles. For the 26 mm and 33 mm corrugations, the corresponding frequencies are much lower than the pinned–pinned resonance, which might be caused by some unexpected sources. It has to be noted that the train velocity is strictly controlled and downslope overspeed will result in braking deceleration. Since the complex rail corrugations mainly occur in downslope small-radius curves, the wheel-rail contact mechanism needs to be further studied. The influence of rail corrugation is further discussed in combination with the dynamic responses of the track in the next section.

In around 2 months after grinding when the grinding marks have been worn out, the rail corrugations of the left line are measured again, and the results are presented in Figure 6 and Figure 7.

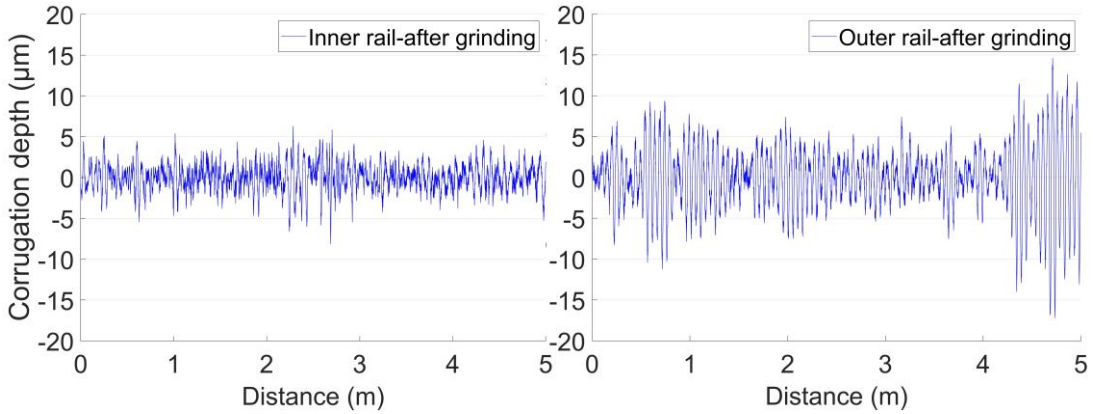

Figure 6: Rail corrugation with the wavelength of 0-100 mm after grinding.

It can be seen that after grinding, the rail corrugations are not eliminated despite no visible marks. The remaining depth of the corrugations on the inner rail and the outer rail are around 10 μm and 30 μm (Figure 6), and the remaining wavelengths on the inner rail and the outer rail are 26 mm and 50 mm (Figure 7), which are respectively the deepest waves in these rails. From this point of view, rail grinding should be performed based on the precise measurement of rail corrugation. The remaining corrugations of this section may still have negative impacts on the dynamic performance of the track.

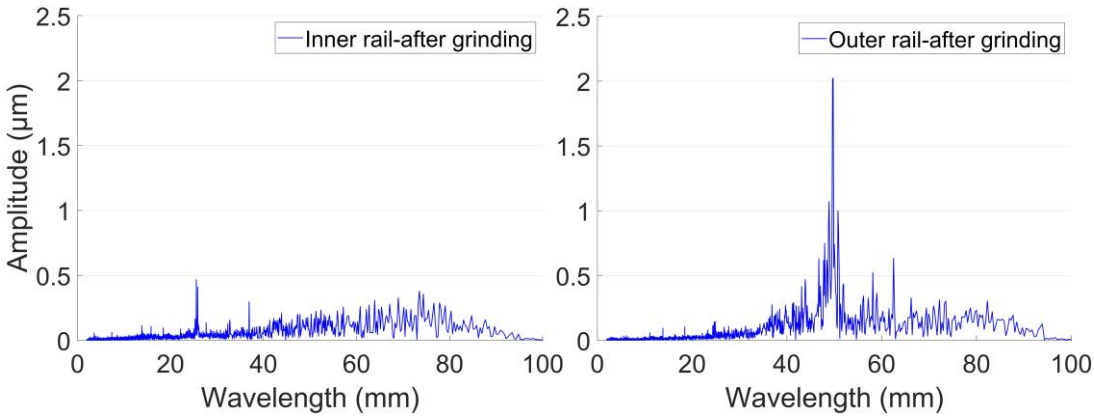

Figure 7: Rail corrugation 0-100 mm wavelength distribution curve after grinding.

3.2 Track dynamic responses

In the field measurements, all the accelerometers are installed on the inner rail side. The rail acceleration responses are given in Figure 8 and Figure 9. It can be seen that for the left line before grinding, the amplitude of rail vertical acceleration is around 1200 m/s^2, which is significantly higher than that of the right line with no corrugation (around 100 m/s^2). Such results reflect the negative impact of the corrugation on the wheel-rail interaction. After grinding, the rail acceleration level of the left line is reduced to around 200 m/s^2.

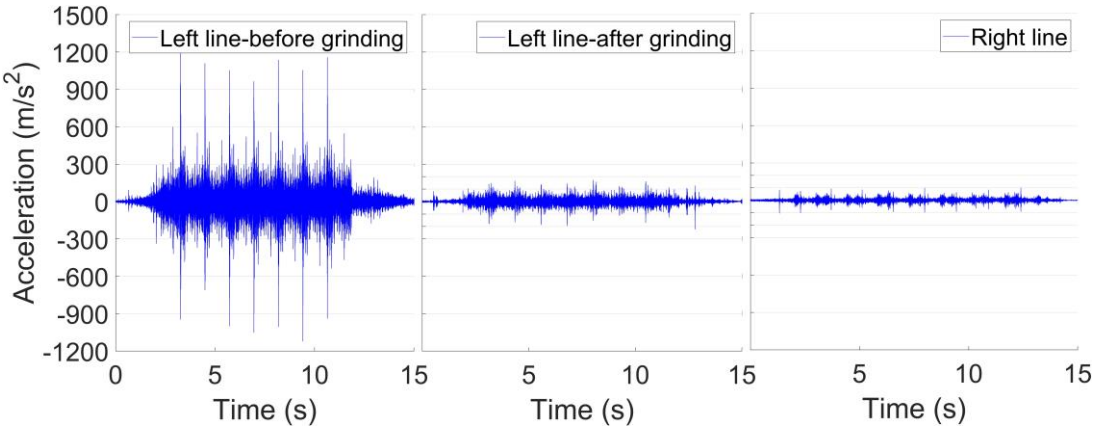

Figure 8: Rail vertical acceleration responses in the time domain in different sections.

The frequency domain responses of the left line before grinding (Figure 9) clearly show four different major frequencies, e.g. 715 Hz, 560 Hz, 430 Hz and 370 Hz. These frequencies are highly consistent with the corresponding rail corrugations. In this case, the corrugation-induced rail vibration dominated the dynamic responses of the rail.

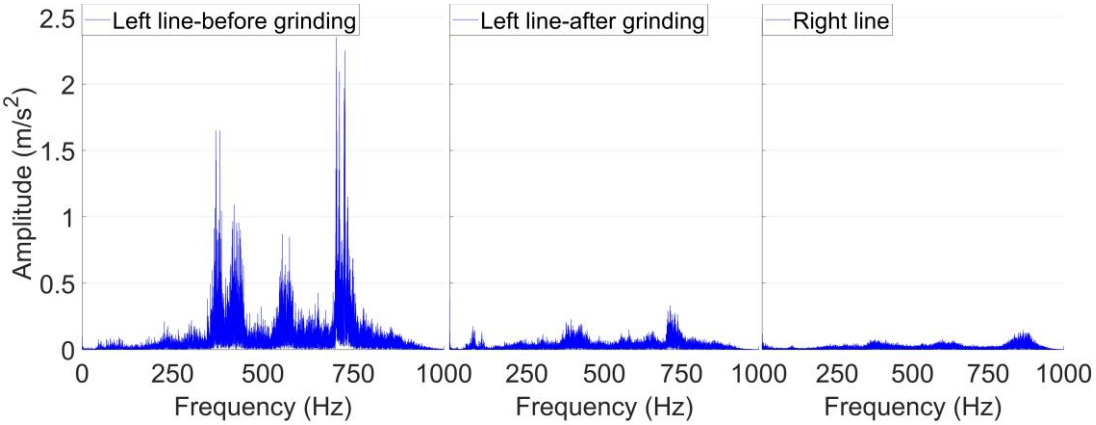

Figure 9: Rail vertical acceleration responses in the frequency domain in different sections.

The negative impact of the rail corrugation is quite serious. Sudden fracture of clips has been frequently reported in this section. The fracture point is mainly in the small arc (Figure 2). In this study, the vibrations of a clip (near the rail vibration test point) in both the toe-end and the small arc are measured. The clip measurement results of the left line before grinding are presented in Figure 10 and Figure 11.

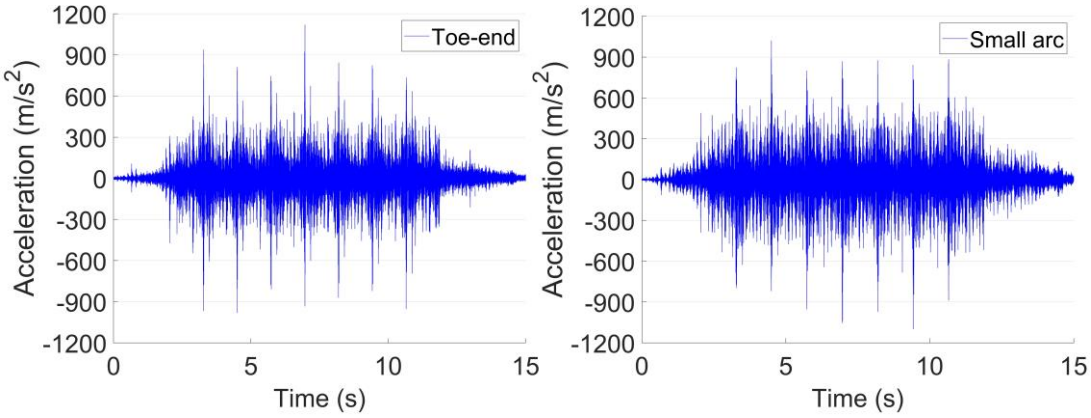

Figure 10: Clip vertical acceleration responses in the time domain in different positions.

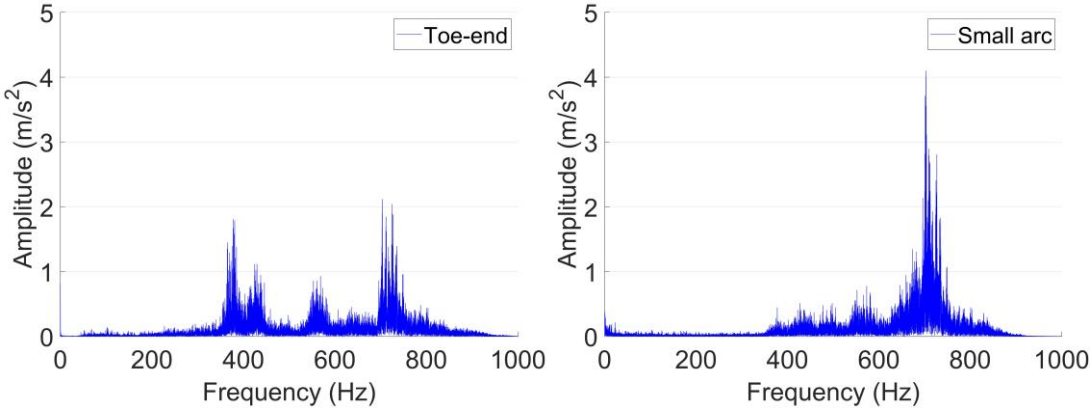

Figure 11: Clip vertical acceleration responses in the frequency domain in different positions.

It can be seen from Figure 10 and Figure 11 that in both test points of the clip, the amplitudes of vibration are at the same level as the rail vibration, but the vibration characteristics in the two points are quite different. In the toe-end, the major vibration frequencies are consistent with those of the rail, which is logical with a buckle pressure of around 12 kN. In the small arc, the only dominant frequency is around 720 Hz excited by the corrugation of 26 mm. Since the inherent frequency of this type of clip is 781 Hz and the sensitive frequency range is 707-798 Hz[11], the corrugation-induced resonance of the clip is likely to be the direct cause of the clip fracture. Considering that the corrugation of 26 mm and clip fracture mainly occurs on the downslope side, the wheel-rail interaction mechanism in such operation conditions needs to be further studied.

Together with the rail and clip, the vibration of the tunnel wall is also measured and recorded simultaneously, and the measurement results are presented in Figure 12. It can be seen that although the excitation frequencies of the rail corrugation in the left line before grinding are above 300 Hz, which are expected to be filtered out by the steel-spring floating slab, the vibration propagated to the tunnel wall (0.08 m/s^2) remains much higher than that of the right line (0.01 m/s^2). After rail grinding, the tunnel wall vibration of the left line is reduced to the same level as the right line.

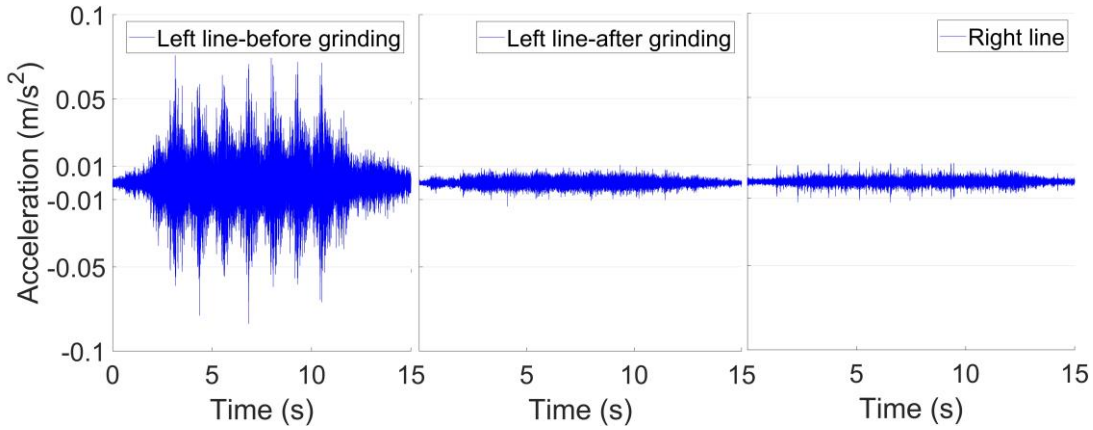

Figure 12: Tunnel wall vertical acceleration responses in the time domain in different sections.

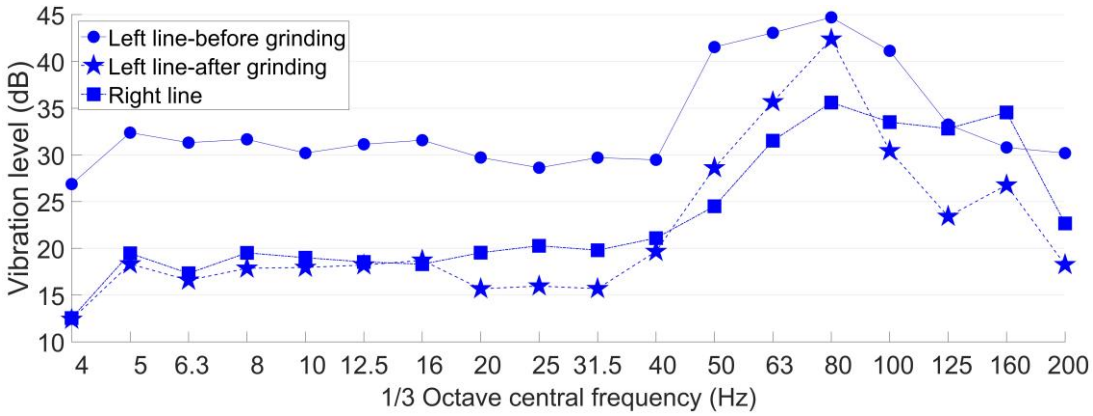

Figure 13: Tunnel wall acceleration responses of different sections in 1/3 Octave spectra.

As presented previously, the vibration level of the tunnel wall in the frequency range of 4-200 Hz is widely used to assess the vibration density of the tunnel lines of urban rail transit, and the key indicator is the maximum vibration acceleration level in 1/3 octave spectra (VL_{max}). The comparison of the tunnel wall acceleration responses of different sections in 1/3 Octave spectra is shown in Figure 13. It can be seen that the corresponding frequency band of VL_{max} is 80 Hz in all the measurement sections. In the left line before rail grinding, the VL_{max} is 45 dB, which is 10 dB higher than that in the right line. In fact, in each band below 100 Hz, the vibration level of the left line before grinding is 10-15 dB higher than that of the right line. After grinding, the vibration level in most of the frequency bands is reduced to the same level as the right line. The adoption of the steel-spring floating slab is to keep the train-induced vibration from transmitting to the environment, while the generation of rail corrugation dramatically reduced such effect.

4 Conclusions and future work

This paper investigated the track dynamic performance of a downslope small-radius curve section. The rail corrugations are measured and analysed, and the influence of

rail corrugations on track damage is further discussed. The main findings can be drawn below.

1. The rail corrugations mainly occur in the downslope side of the small-radius curve section (left line), and it is more complicated on the inner rail than on the outer rail. Considering that the corrugation-induced excitation frequencies of 535 Hz and 719 Hz are not related to the pinned-pinned resonance or the second torsional resonance of driven axles, a possible explanation could be the complex wheel-rail interaction in the downslope small-radius curve due to the speed control mechanism.

2. The excitation frequency of the shortest wavelength (26 mm) on the inner rail is within the clip-sensitive frequency range (707-798 Hz). This corrugation wavelength is likely to be the direct cause of the clip resonance fracture in this section.

3. Despite the excitation frequencies being relatively high (374-719 Hz), the vibration propagated to the tunnel wall in the frequency range of 4-200 Hz is also dramatically magnified for more than 10 dB, which largely weakened the vibration control effect of the steel-spring floating slab.

This study is a periodic summary of the investigation of track damage on the downslope small-radius curve. In the next step, the wheel-rail interaction mechanism in such sections based on the train operation mechanism will be further studied, and possible treatments to control the development of rail corrugation will be proposed.

References

[1] Yoshihiko Sato, Akira Matsumoto, Klaus Knothe. Review on rail corrugation studies. Wear. 2002, 252(1-2): 130-139.

[2] Xuesong Jin, Xia Li, Wei Li, et al., Review of Rail Corrugation Progress. Journal of Southwest Jiaotong University. 2016, 51(2): 264-273.

[3] A. Saulot, S. Descartes, D. Desmyter, et al., A tribological characterization of the “damage mechanism” of low rail corrugation on sharp curved track. Wear. 2006, 260(9-10): 984-995.

[4] Akira Matsumoto, Yasuhiro Sato, Hiroyuki Ono, et al., Formation mechanism and countermeasures of rail corrugation on curved track. Wear. 2002, 253(1-2): 178-184.

[5] Z. Wang, Z. Lei, J. Zhu, Study on the formation mechanism of rail corrugation in small radius curves of metro. Journal of Mechanical Science and Technology. 2023, 37(9): 4521-4532.

[6] Zhiqiang Wang, Zhenyu Lei, Trend analysis of rail corrugation on the metro based on wheel–rail stick-slip characteristics. Vehicle System Dynamics. 2024, 62(1): 147-176.

[7] Zhenyu Lei, Zhiqiang Wang, Contact and creep characteristics of wheel–rail system under harmonic corrugation excitation. Journal of Vibration and Control. 2021, 27(17-18): 2069-2080.

[8] ISO 2631-1:1997, Mechanical vibration and shock – Evaluation of human exposure to whole-body vibration – Part 1: General requirements, 1997.

[9] A.P. de Man. Dynatrack: a Survey of Dynamic Railway Track Properties and Their Quality. PhD Thesis, Delft University of Technology, 2002.
[10] S.L. Grassie, Rail corrugation: characteristics, causes, and treatments. Proceedings of the Institution of Mechanical Engineers, Part F: Journal of Rail and Rapid Transit. 2009, 223(6): 581-596.
[11] Chengliang Yang, Analysis of Fracture Reason of DT-III Type Fastener Clip. Master Thesis, China Academy of Railway Sciences, 2019 (in Chinese).